Combustion of a substitution fuel made of cardboard and polyethylene : influence of the mix characteristics -experimental approach

Sylvain Salvador, Michel Quintard, Céline David

Combustion of a substitution fuel made of cardboard and polyethylene: influence of the mix characteristics—experimental approach

S. Salvador[a,*], M. Quintard[b], C. David[a]

[a]*École des Mines d'Albi-Carmaux, Laboratoire de Génie de Procédés des Solides Divisés, UMR 2392 CNRS, Campus Jarlard, route de Teillet, Albi CT, Cédex 09 81013, France*
[b]*Institut de Mécanique des Fluides de Toulouse-UMR 5502 CNRS, Allée du Pr Camille Soula, 31400 Toulouse, France*

Abstract

This article presents an experimental study of the combustion of substitution fuels elaborated from compressed mixes of cardboard and polyethylene (PE). These components are representative of two classical classes of waste materials: materials derived from wood and plastics. The combustion of these fuels has been experimentally characterized in terms of combustion rate, and quantity of PolyAromatic Hydrocarbons (PAH) pollutants emitted. The temperature levels reached within the fuel sample are also reported and discussed. A parametric study has been performed with three characteristics of the fuel as the parameters: (i) the size of the elements before mixing; (ii) the proportion of PE in the mix; (iii) and the apparent density of the 'bricks' that were prepared.

Experiments were conducted using a standard calorimeter cone. This device leads to a quasi-1D situation, and good repeatability has been observed. A special sample holder and a PAH sampling system were adapted to the system. The samples were irradiated with a flux of 50 kW m^{-2}. No air was blown through the samples, and the ash layer formed at the surface was not removed.

It was observed that combustion occurs with two different stages. During the first stage, the fuel is devolatilized, and a flame is formed at the surface. It was observed that the duration of this period was proportional to the fuel density. The mass loss rate (kg s^{-1} m^{-2}) appeared not to depend upon the brick characteristics. In second stage, the fuel is oxidized. The mass loss rate is again very similar from one brick to another. It is approximately 10 times smaller than during the devolatilization stage.

An examination of the temperature levels at three locations inside the bricks indicates that there is not a thin combustion front propagating through the sample. As a consequence of this, despite the large quantity of energy released by the combustion, the temperature reached remains between 700 and 900 °C, which is very close to the surface steady state temperature resulting from the surface irradiation.

PAHs are formed during the flame period. The PAH specified here are those formed inside the flame at the brick surface. In the case of an industrial application, it must be emphasized that these PAHs are likely to react downstream depending on the furnace conditions.

The density of the fuel and the size of the elements have no impact on these emissions. Our results show that this is the percentage of PE that controls the emissions. We showed that the introduction of more than 30% of PE (expressed in micrograms per gram of PE) leads to very high PAH emissions. Moreover, for mass fractions of PE larger than 30%, heavy PAH, which are more toxic than light PAH, are formed in majority.

In conclusion, if PE mass fractions lower than 30% are used, such substitution fuels allows one to recover the available energy of these materials, while solving the environmental and technical problems usually encountered when burning these materials individually.

Keywords: Substitution fuels; Cardboard; Polyethylene; Combustion; Polyaromatic hydrocarbons; Calorimeter cone

1. Introduction

The development of substitution fuels by mixing materials coming from very different sources is a way to recover their energy, while offering a great potential for the improvement of waste incineration in terms of material storage and transport, process control and environmental impact of the operations. Many different mixes have been investigated, as well as different combustion processes [1–4]; see also the review on co-combustion by Rasmussen et al. [5]. This article considers only mixes made of plastics and wood derived materials.

* Corresponding author. Tel.: +33-5-63-49-30-00; fax: +33-5-63-49-30-99.
E-mail address: salvador@enstimac.fr (S. Salvador).

The combustion of a bed where plastic materials are present in high concentration will result in the formation of large quantities of polyaromatic hydrocarbons (PAH) in the exhaust gas [6,7]. This is a very important issue because of the high toxicity of these species. In addition, problem arises during the combustion of plastic materials alone because of the possible occurrence of melting, during which the material will flow through the grids of the incinerator, or stick to some parts of the plant (feeders, walls). By mixing and compacting them with wood derived materials such as paper, cardboard or wood chips, one can prepare fuels of different sizes and forms, e.g. pellets, bricks or 'ballots', and solve the last two above-mentioned problems. Following Liu [1], 'using a mixture of paper and plastic film as fuel can overcome the problem of low combustion efficiency of the plastic and make use of its high heating value'.

This practice has additional advantages. Wood derived materials and plastic materials have a very low apparent density when stored as a waste. The compaction largely reduces their volume, making effective storage, mechanical handling and transport easier. Liu et al. [1] made a detailed study of the compaction of such mixes in order to control their density, their mechanical properties such as abrasion and impact resistance. They also determined their combustion characteristics, such as the Higher Heating Value and the proximate analysis. The risks regarding fire are also largely reduced. If one considers the control of the humidity and of the lower calorific value (LCV), it becomes possible to use seasonal materials with different LCV and adjust the LCV of the mix through the used proportions. Finally, grinding, mixing and compacting allow one to adapt waste and biomass materials to different incineration processes: beyond the size of the fuel pieces that can be adapted to the process, the 'combustion velocity' can be *controlled through the making parameters* that will be detailed below. This solves the problem of the very rapid combustion of these materials each time a non-compacted quantity is fed, which causes difficulties in the incinerator monitoring. It is shown in Fig. 1 some examples of bricks made of wood derived and plastic materials.

This article deals only with the combustion of a substitution fuel elaborated from cardboard and polyethylene (PE). Cardboard and polyethylene were chosen primarily because they are very frequent waste materials. Indeed, large quantities of these materials are generated by the packaging industry, and are more and more used as fuel in small-scale applications [2]. They are also representative of the two classes of materials discussed in this section, namely, wood derived materials and plastics.

The influence on the combustion processes of three making parameters entering in the preparation of mixes of cardboard and polyethylene has been characterized experimentally: the element size of the mix, the proportion of PE, and the density.

(i) The element size will affect the mixing of the volatile species generated by the two components. It is one goal of this work to establish whether this parameter has an impact on the nature of the combustion products, with a particular interest for PAH emissions. For instance, by studying the pyrolysis—first step of the combustion of a solid fuel—of mixes of different cellulose components, Lewin et al. [8] showed that there were interactions between the gas species coming from the different components.

(ii) The proportion of PE in the mix may affect the PAH emissions. Previous works showed that, regarding PAH emissions, a maximum mass fraction of approximately 5% of PE could be recommended [2]. In a study of copyrolysis of poly(vinylchloride) with cellulose derived materials, McGhee et al. [9] showed that the char (solid carbon residue) yield is greater than those produced by pyrolysis of the individual components. They argue that the presence of chlorinated polymers is at the origin of these interactions. Williams et al. [10] showed that the pyrolysis of 'Mixed Plastics' leads to changes in the amount of PAH produced compared to that expected from the individual plastics.

Fig. 1. Some examples of bricks from wood derived and plastic materials (with the agreement of: RUF^{R} Briquetting Machinery).

Table 1
Ultimate analysis, proximate analysis and lower calorific value (LCV) for the cardboard and for the polyethylene

	Ultimate analysis (% mass)					Proximate analysis (% mass)		LCV (kJ kg^{-1})
	C	H	O	N	S	Volatile matter	Ash	
Cardboard	38.72	5.59	40.37	0.46		69.1	5.6	15,425
Polyethylene	86	14	–	–	–	100	–	42,978

(iii) It is expected that the density of the mix will control the combustion velocity. In turn, this can have an effect on the nature of the combustion products.

The moisture of the mix may also have an impact on the combustion rate, and potentially on the final combustion products. For simplification purposes, this factor has not been studied here.

This article presents an experimental parametric study of the combustion of cardboard/PE bricks. The bricks were prepared by grinding the two materials separately, mixing them, and compacting the mix. The combustion was operated in a quasi-1D situation, with a free flame at the top surface. This was achieved by adapting a calorimeter cone—a standard test experiment for the investigation of plastic materials ignition and combustion velocity—to the combustion of porous materials with large thickness, such as the bricks developed in this work. No air was forced through the sample (brick), and the char residue and ash formed at the surface were not removed. Under these conditions, the experiments may be used to model the combustion progress on an *elementary surface* of any solid of the same composition and density.

The three making parameters discussed above were changed independently, and their impact was assessed on the following combustion parameters: flame duration, total mass loss rate, temperature levels inside the sample body, and total quantity of PAH formed during the combustion. Such a parametric study has not been reported before. Nevertheless, mention should be made of the work by Keränen et al. [2], who characterized the emissions from wood and plastic wastes combustion in residential furnaces, varying the composition of the fuel and overall combustion conditions.

2. Experiments

2.1. Materials

The cardboard used in this study was chosen to represent a typical sample among the large variety of material that can be found on the market. It is a classical corrugated cardboard with a wavy layer between two flat paper layers. The ultimate and proximate analyses of the dried product are given in Table 1, together with its LCV. The natural moisture, when stored in the laboratory, was measured to be about 7% wet-basis. The volatile matter was found to be high at 69.1%, and the ash content was measured at 5.6%. All the percentages here and in the sequel of the paper correspond to mass fractions. From the ThermoGravimetry (TG) curve in Fig. 2(a), it can be seen that the thermal degradation under N_2 is rapid at temperatures between 280 and 370 °C, and then slower.

A very low-density polyethylene, normally used as packaging film, was taken as the plastic material. It is

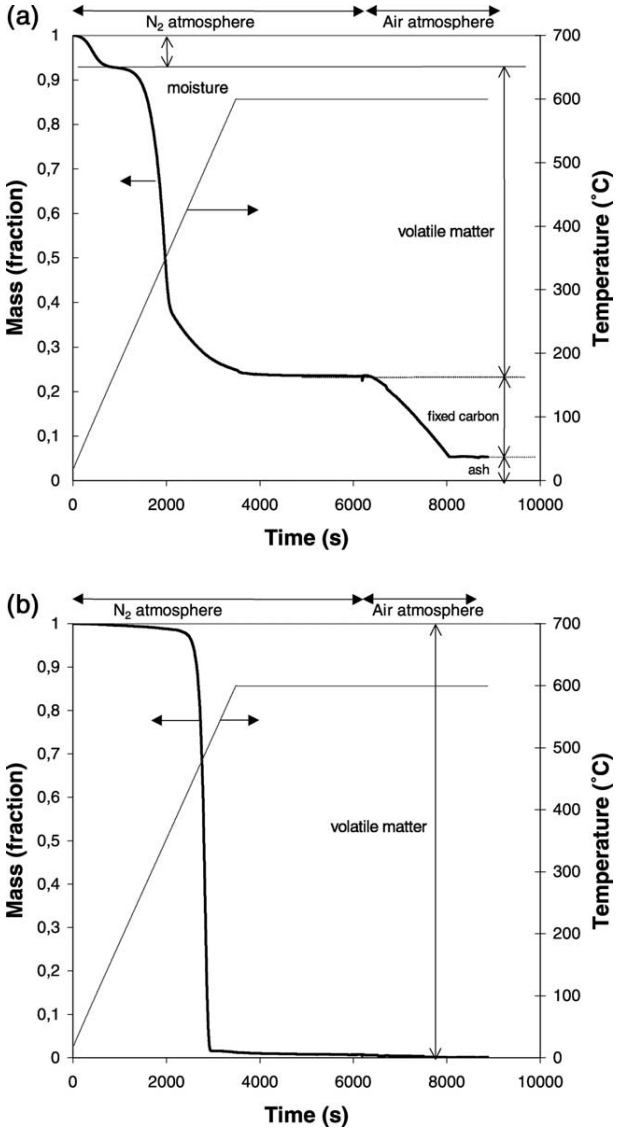

Fig. 2. (a) ThermoGravimetric curve for the cardboard. (b) ThermoGravimetric curve for the Polyethylene.

denoted PE throughout the article. From its analysis as reported in Table 1, it can be seen that the PE has no solid residue after devolatilization (heating under N_2) and leaves no ash after oxidation (under air). This is confirmed by the TG curves presented in Fig. 2(b): the devolatilization occurs very rapidly, at temperatures between 440 and 515 °C.

For a better repeatability, the two materials used in this study were clean 'fresh' materials, and not real wastes that could have been contaminated by paints, stickers, or ink.

2.2. Making of the bricks

Cardboard and PE were ground using a blade grinder fitted with a perforated grid at its bottom. The diameter of the grid holes could be 8, 20 and 40 mm. Since a well-defined particle size distribution cannot be easily realized on such materials, we use the diameter of the grid holes to characterize the size of the ground elements. Of course, some pieces could be larger or smaller, and the geometry is not well-controlled.

Mixes were prepared by compacting known masses of each component in a fixed volume, thus giving a known brick density. Compaction was obtained inside a cylinder fitted with two pistons that were moved simultaneously along the axis. This leads to relatively good homogeneity in the brick density. After compaction, the brick is expulsed from the cylinder using a long 'piston', and forced inside a stainless steel belt. A stainless steel grid (2 mm diameter wire, 20 mm step) was placed on each flat surface of the sample. This packaging was necessary to ensure a stable density of the brick during storage and experiments. The final size of the bricks is 100 mm in diameter and 50 mm in height. Fig. 3 shows examples of brick samples.

Parameters for the making of the bricks are summarized in Table 2a. The reference brick was composed of 20 mm elements, contained 20% of PE, and was compressed at

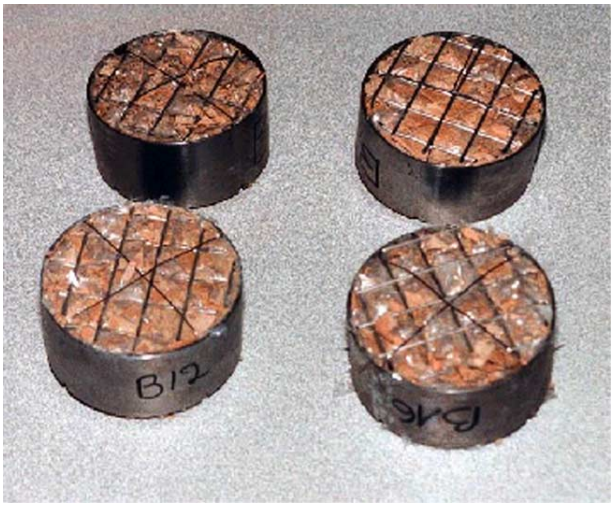

Fig. 3. Photograph of a brick inside the stainless steel belt and fitted with two surface grids.

Table 2a
Range of variation for the three making parameters of the bricks: density, percentage of PE, and size of the elements

Density	Mass fraction of PE (%)	Size of the elements (mm)
	0	
	5	
300	10	8
500	20	20 (reference brick)
700	33	40
900	70	
	100	

500 kg m^{-3}. Subsequently, only one parameter was changed at a time for each brick (as compared with the reference). The parameters for the different experiments are listed in Table 2b.

Three other densities have been tested: 300, 700 and 900 kg m^{-3}. The lower value was fixed at 300 kg m^{-3} because of mechanical holding reasons. Indeed, below this value, the brick would easily fall apart even with careful handling. At such a density, it is easy to compress further by pressing the brick surface with the finger. On the contrary, the brick at a density of 900 kg m^{-3} is very hard. A strong pressure from the nail would only mark the surface. This brick, even without the steel belt and grids, can be handled without falling apart. This was also the case for the bricks at 500 and 700 kg m^{-3}. It should be noticed that this density is similar to that of natural wood. The pressure to reach the different densities can be estimated from Fig. 4, where we have plotted the density versus the compaction pressure applied to the brick surfaces. The brick at 900 kg m^{-3} requires a pressure greater than 5×10^8 Pa. This pressure decreases by more than two decades for a density of 300 kg m^{-3}.

The *percentage in PE* was varied between 0 and 100%. The two extreme values, corresponding to pure cardboard and pure PE, will serve as references for the discussion.

Table 2b
Parameter values for all the experiments

Experiment	Density (kg m^{-3})	Mass fraction of PE (%)	Size of the elements (mm)
#1	300	20	20
#2	500	20	20
#3	700	20	20
#4	900	20	20
#5	500	0	20
#6	500	5	20
#7	500	10	20
#8	500	20	20
#9	500	33	20
#10	500	70	20
#11	500	100	20
#12	500	20	8
#13	500	20	20
#14	500	20	40

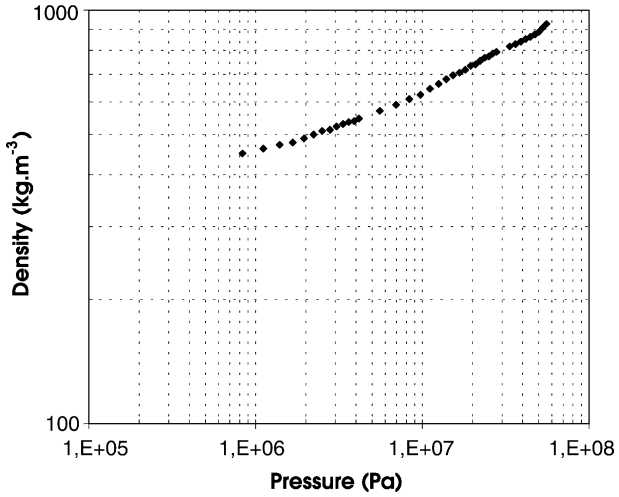

Fig. 4. Density of the mix (80% cardboard, 20%PE) versus the compaction pressure.

The size of the ground elements was varied between 8 and 40 mm. The size of 40 mm was considered as the maximum acceptable with respect to the diameter of the bricks. It is also estimated that sizes below 8 mm have less industrial interest, and would cause difficulties with the brick holding.

2.3. Combustion experiments

The combustion was operated in a calorimeter cone. This test device is commonly used today to characterize the ignition delay and combustion rate of plastic materials submitted to a surface radiative flux. It has been precisely described [11] and standardized (ISO 5660 standard).

The principle is illustrated in Figs. 5 and 6. An electrically heated resistance is coiled to a cone shape. The shape of the heater is designed to impose a spatially constant radiative flux on the surface of the tested sample placed 50 mm below, this surface having a typical dimension 100 mm by 100 mm. The heater temperature is monitored to ensure a constant value of the heat flux, ranging between 25 and 100 kW m^{-2}. This radiative flux will heat the sample surface, inducing its devolatilization. The gases will ignite by self-ignition, or thanks to an optional electrical spark igniter. A flame is formed at the surface of the sample, and may develop through the cone. After this, the combustion of the sample will progress. A load cell, as shown in Figs. 5 and 6, is used to continuously record the total mass of the sample.

A strong airflow, 24 l s^{-1} @ 20 °C, is sucked through the top hopper. The flow rate is measured via a diaphragm flow meter, and it is maintained constant during the test. The airflow rate is very high, so that the combustion is always under large bulk equivalence ratio. Quantitative information about this point will be given later. The mix of air and of the combustion flue gas is sampled for gas analysis. The classical gas analysis that are made on a calorimeter cone, e.g. O_2, CO_2 and CO are not considered, but we will consider only the analysis of PAH emissions. A special sampling and capture system has been developed to this purpose (Fig. 6). Gases are iso-kinetically sampled inside the main air duct, and filtered on a 0.3 μm filter. The gas sample then crosses a 50 mm thick bed of XAD-1180 resin that captures the lighter PAHs. After the end of an experiment, the resin and the filter are desorbed and PAH are quantified by high performance liquid chromatography. The procedure follows the recommendations of the AFNOR 11338-1 standard.

Temperatures inside the bricks were measured using three refractory, steel-protected chromel/alumel thermocouples inserted 5, 25 and 45 mm below the sample surface. They were introduced along a radius through the sample holder and inside the brick. It was necessary to run specific experiments for temperature measurements since the thermocouples were disturbing the weighing system.

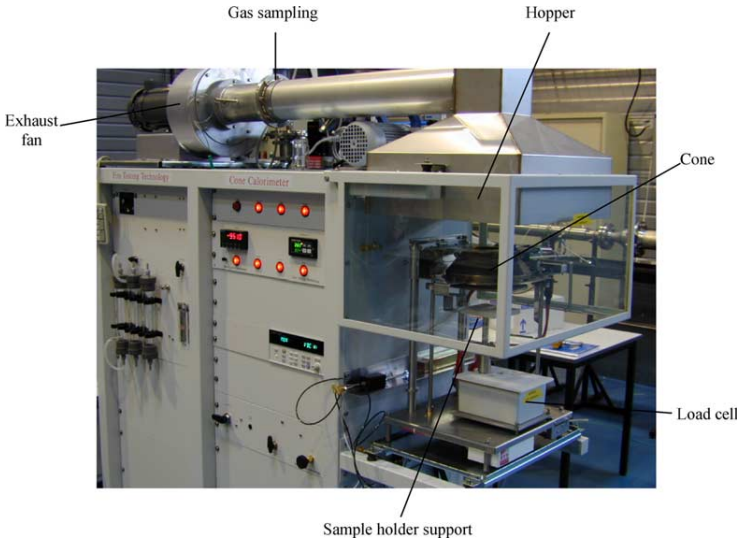

Fig. 5. Photograph of the Calorimeter Cone. The sample holder and the brick have been removed.

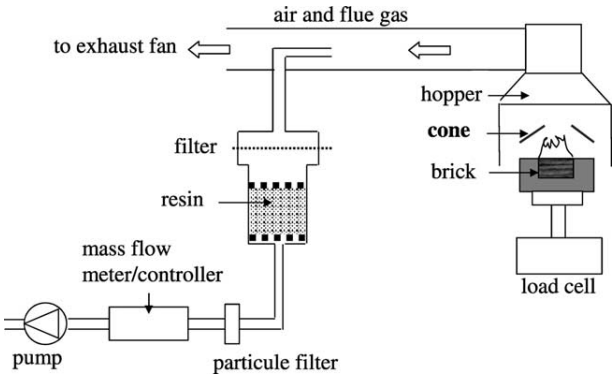

Fig. 6. PAH capture experimental setup.

We have replaced the standard sample holder, originally designed for plates several mm thick, by a holder specially designed for the bricks. It consists of a refractory, low heat conductivity material that surrounds the brick lateral surface and bottom (see Fig. 7). The holder was designed to obtain a quasi-1D combustion process, starting from the top surface of the brick and propagating towards the bottom. The possibility of obtaining a 1D front was one of the arguments to retain the calorimeter cone as the tool to perform our experiments, with the perspective of future modeling of the combustion inside the brick.

For all experiments reported here, the radiative heat flux imposed at the sample surface was 50 kW m^{-2}, corresponding to a cone temperature of 1017 K. If one makes the parallel with combustion in industrial processes, this flux simulates radiation from other burning solids and from the chamber walls. The spark igniter was used since it had the advantage to ensure a good repeatability of the ignition delay.

3. Results and discussion

In this section, we describe first a typical experiment with the 'reference brick', and then explore the influence of the various parameters.

Fig. 7. Photograph of the sample holder and of a brick.

3.1. Description of an experiment: case of the reference brick

The sample is placed inside the sample holder and on the load cell, below the heater cone, while a shield stops the cone radiation. At time $t = 0$, the shield is removed and the experiment starts. The surface is rapidly heated and the cardboard and PE start to devolatilize. After a delay of typically 4 s, a flame ignites. Its height is about 200 mm at the beginning, then it decreases to a few centimeters after about 6 min. After half an hour, the flame intensity increases again, and finally stops at about $t = 1$ h. Following this devolatilization period, the char residue starts to oxidize. Nothing much can be observed except a localized, several millimeters thick flame moving at the sample surface. The period for char oxidation lasts for more than 3–4 h. Nevertheless, experiments were stopped before the end of the combustion as the ash layer that formed at the surface started to collapse under its weight. This occurs approximately after two times the duration of the devolatilization period. Inside an industrial process, a too thick ash layer would be removed by the handling systems, or because of the airflow, or else, due to mechanical interactions between the fuel pieces. The final combustion stage, that would be controlled by ash removal, was not of interest in this study.

3.2. Influence of the brick density

Fig. 8a plots the total mass evolution for the four bricks with the different densities tested in this work. We have indicated with an 'x' symbol the date when the volatile flame stops. The mass evolution for the 500 kg m^{-3} brick indicates a rapid decrease in the period 0–3000 s. This period corresponds to the flame period (combustion of the volatile matters). The duration of this flame period largely depends upon the density, and appears to be proportional to the density as illustrated in Fig. 9. The duration of the flame reaches 1.5 h for the brick at 900 kg m^{-3}. These results are of great interest for industrial applications since they indicate that *one may act on the density in order to control the volatile flame duration*.

Fig. 8a shows that the mass loss rate, represented by the slope of the curves, is very similar from one experiment to the other. The average rate, based on one m^2 of brick surface, is about 6.2×10^{-3} kg s^{-1} m^{-2}. It is difficult to interpret these results in terms of the involved phenomena. Indeed, this behavior is the result of a complex interaction between heat transfer by conduction in the solid matrix inside the brick, convection of the volatile matter inside the brick, and the kinetics of the devolatilization reactions.

A quantification of the global bulk equivalence ratio for the combustion, denoted Φ, can be established at this stage.

$$\Phi = \frac{\frac{m_{\text{fuel}}}{m_{\text{air}}}\text{actual}}{\frac{m_{\text{fuel}}}{m_{\text{air}}}\text{stoichiometric}} \tag{1}$$

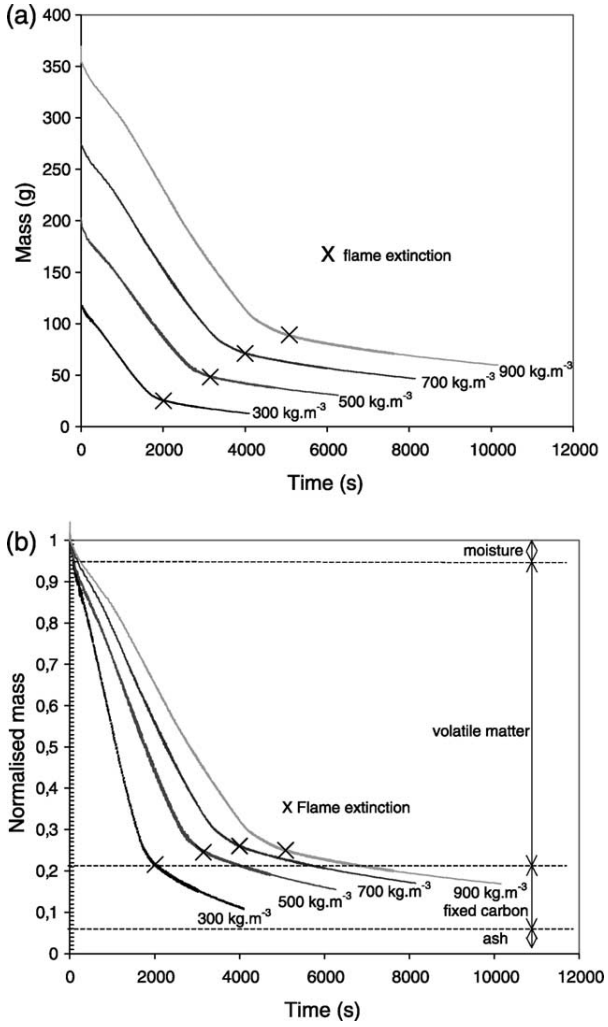

Fig. 8. (a) Total mass evolution for the four bricks with different densities. The date of flame extinction has been located. The element size is 20 mm, and the mass fraction of PE is 20%. (b) Normalized total mass evolution for the four bricks with different densities. The date of flame extinction has been located. The element size is 20 mm, and the mass fraction of PE is 20%.

The maximum mass loss rate for the bricks was $4.9\ 10^{-5}$ kg s^{-1}. The air flow-rate was 24 l s^{-1} @ 20 °C, which is equivalent to 0.0278 kg s^{-1} ($\rho_{air} = 1.16$ kg m^{-3}). On the basis of 11 kg air kg fuel^{-1} for a stoichiometric combustion, the bulk equivalence ratio was circa 51. The combustion is therefore globally under very large air excess. Nevertheless, it is *the presence or not of air inside the flame zone that will affect the PAH formation*. This value is not measurable during the combustion of large solid bodies.

A plot of the time evolution of the brick mass normalized to the initial mass is shown in Fig. 8b. It greatly helps in interpreting the results. The date for the flame extinction, together with the moisture, the volatile matter content and the ash content of the mix, 5.6, 75.3 and 4.5%, respectively, are reported on this figure. This shows that, for all the bricks, some volatile matter is still left when the flame stops.

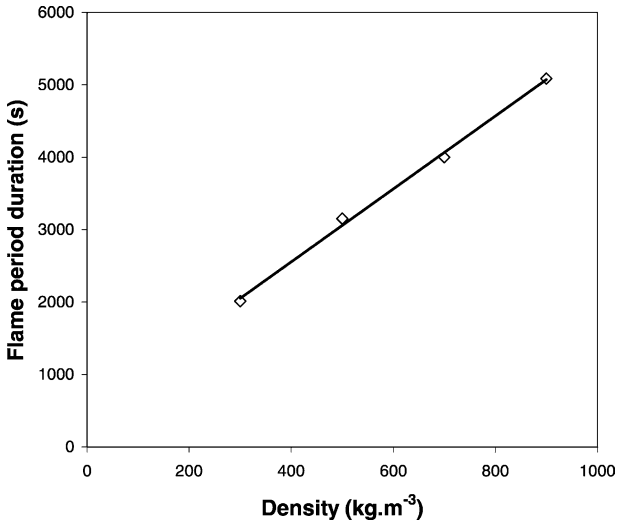

Fig. 9. Duration of the volatile flame versus the density of the brick. The size of the elements is 20 mm, and the mass fraction of PE is 20%.

The two phases of devolatilization and char oxidation are therefore overlapping during a short period.

During the char oxidation phase that follows, the mass loss rates are much smaller than during the devolatilization phase, and they are also similar from one experiment to another (Fig. 8a). The average value is 0.6×10^{-3} kg s^{-1} m^{-2}, which is approximately 10 times smaller than during the devolatilization.

It is important to note that the repeatability of the mass information has been checked and that we found that the differences between two experiments were always less than 3%.

The temperatures reached inside the brick are given in Fig. 10a–d. The temperature at a location 5 mm below the surface increases rapidly. The more compact the brick, the less rapid is the heating. This temperature reaches a stable level after 2000 s for the brick at 300 kg m^{-3} and 6000 s for the brick at 900 kg m^{-3}. The time to reach this temperature stabilization corresponds approximately with the flame duration. It can be concluded that char oxidation occurs at a quite constant temperature with respect to time. The observed stable temperature levels are the same when the density varies, with values between 700 and 900 °C. The breakdown in the curves for the measurement close to the surface is linked to mechanical problems: once the char oxidation has advanced, the thermocouple located in the ash is not sufficiently maintained and can move towards the interior of the brick or above the surface.

For all the temperature curves, and whatever the brick density, we observed clearly a small plateau when the temperature reaches approximately 100 °C. This can be attributed to the drying mechanism inside the measurement zone. A less marked stage is observed at a temperature of 500 °C. It corresponds with the PE peak devolatilization temperature as indicated by the TG analysis. This reaction is

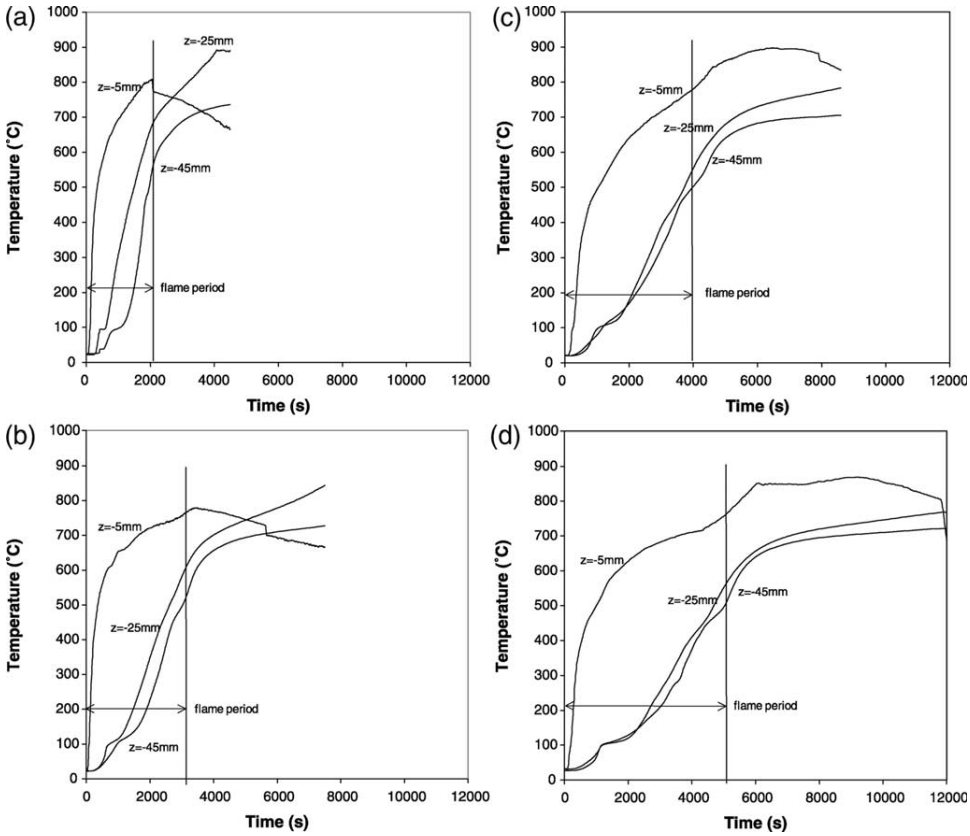

Fig. 10. Temperature evolution inside the brick body (a) 5 mm below the surface; (b) 25 mm below the surface; (c) 45 mm below the surface.

more rapid than the cardboard devolatilization. As a consequence, this last reaction does not induce a marked temperature plateau.

The temperatures 25 and 45 mm below the surface increase less rapidly as expected. All the curves tend to stabilize to values between 700 and 900 °C. This temperature corresponds to the steady state temperature of the surface that is irradiated by the heated cone. It can be concluded that, despite of the high quantity of heat released by char oxidation, the reaction is slow enough so that the temperature does not exceed the surface temperature by more than 100 °C.

From these low heating rates, it can also be concluded that *there is not a sharp combustion front* propagating through the brick, as it is the case when air is blown through the medium [12]. The presence of a sharp front would also be materialized by an important temperature increase followed by a rapid decrease, which is not observed in our experiments. The absence of a clear oxidization front has also been confirmed by interrupting a test during this stage, and observing the two parts of the vertically cut brick. It is likely that the combustion in our experiments is limited by oxygen diffusion from the top of the brick, and testing this assertion will be one of the objectives of future numerical modeling.

3.3. Influence of the element sizes

We now investigate the influence of the size of the elements after grinding. The range of variation, as previously stated, is between 8 and 40 mm. Fig. 11 shows the time evolution of the normalized mass of bricks with different element sizes. These results indicate that this parameter does not impact significantly on the mass evolution. The mass loss rate during the devolatilization phase is slightly increasing when the size of the elements is increasing. This might possibly be explained by a change of the thermal conductivity of the media, that is likely to be higher in the case of large pieces of cardboard and PE than in the case of small pieces, because of a different arrangement of the different phases.

The slopes of the mass evolution curves in the char oxidation phase are very similar. This indicates that changes in the porous medium structure do not affect the reaction progress.

3.4. Influence of the percentage of PE

In Fig. 12, we have plotted the time evolution of the normalized mass of bricks containing different PE quantities, ranging from pure cardboard to pure PE. Whatever the PE percentage between 0 and 70%, the

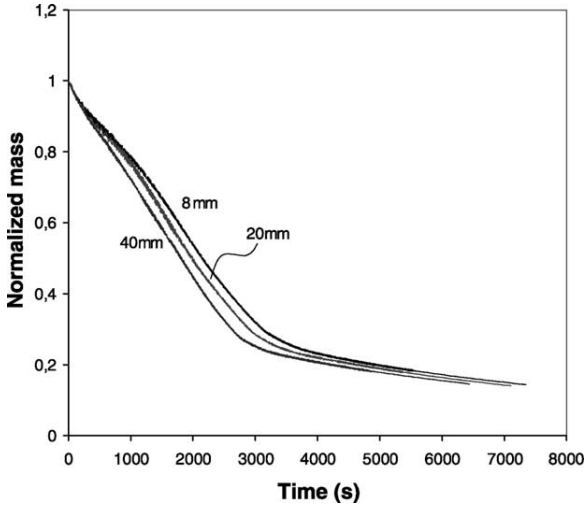

Fig. 11. Normalized total mass evolution for the bricks with different size of the elements. The mass fraction of PE is 20%, and the density is 500 kg m^{-3}.

mass loss rate during the devolatilization phase remains approximately the same.

The differences in the mass loss after devolatilization are due to the differences in the fixed carbon (char) proportion resulting from the various percentages in cardboard. The brick at 100% PE exhibits a very different behavior. Attention should not be paid to this result since the surface of this brick did not remain flat along the test. In fact, we clearly observed that flow of melted PE was occurring. The brick also collapsed near the steel belt, and a 'bump' was formed near the brick center.

For the char oxidation phase, the curve slopes are similar from one brick to another. The chars left after the devolatilization stages have very different densities, since the initial percentage of PE were very different.

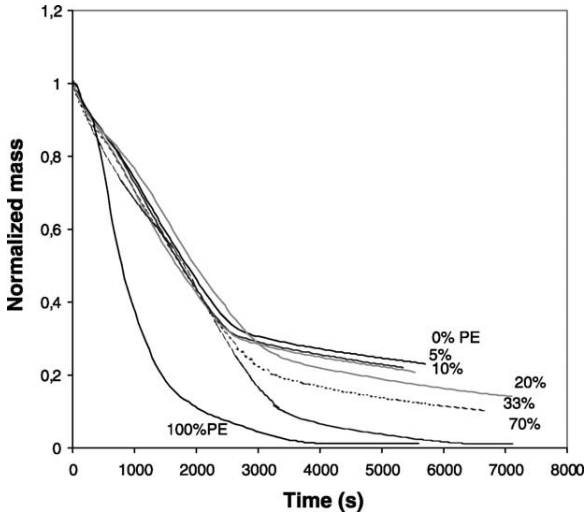

Fig. 12. Normalized total mass evolution for the bricks with different PE percentages. The size of the elements is 20 mm, and the density is 500 kg m^{-3}.

Despite of this, the global oxidation rates for the whole brick are similar. If one wanted to explain this result, one should take into consideration heat transfer and the impact on the local temperatures, oxygen transfer through the porous medium, and chemical reaction kinetics. This cannot be done without the help of a numerical model.

As far as the question of a possible flow of melted PE down the brick is concerned, this work indicated that PE did not flow within the cardboard elements. This could be observed by interrupting a test during the devolatilization stage, and cutting the brick into two parts on a vertical plane. Even in the zone separating the devolatilized part on the top and the non-devolatilized part at the bottom of the brick, the melted PE was present, and did not impregnate the cardboard pieces.

4. Study of PAH emissions

The emission factors of mixes have received some attention in the literature. Ross et al. [4], for instance, have observed pollutant emissions for mixes of coal and biomass lower than those calculated additively.

Literature concerning the combustion emissions of the materials under consideration in this article is poor. Freeman [13] reported the value of 173 μg g cardboard^{-1} for the combustion of cardboard in 'industrial furnace' combustion. Piao [6] quantified the emission during the combustion of PE of the same PAH as those quantified in this work. He reported values between 1600 and 52,000 μg g PE^{-1}. Panagiotou [7] studied the combustion of PE particles inside a reactor where he could control the bulk equivalence ratio. He reported values ranging between approximately 9000 and 21,500 μg g PE^{-1}.

It is hazardous to make comparisons between the values reported by different authors, since the quantity of PAH formed during the combustion is strongly dependent upon different parameters. First, the local richness conditions, which depend themselves upon the mixing efficiency between volatile matters and air, play an important role in PAH formation. In addition, the temperature levels in the flame zone will affect the formation and destruction reaction kinetics [7,14,15], and also H_2 concentrations [16]. Nevertheless, these results clearly indicate that much larger PAH quantities are emitted for PE combustion than for cardboard combustion.

In this work, we have quantified the emissions for the species listed as the most important ones by the United States Environment Protection Agency, e.g. naphthalene, acenaphthylene, acenaphthene, fluorene, anthracene, phenanthrene, fluoranthene pyrene, benzo(a)anthracene, chrysene, benzo(b)fluoranthene, benzo(k)fluoranthene, benzo(a)pyerene, benzo(ghi)perylene, indeno(123-cd)pyrene and dibenzo(ah)anthracene.

As a first investigation, we have quantified the *total PAH emissions* for the combustion of the brick. We have

also quantified the PAH cumulative emissions for the two stages that were observed, e.g. during the volatile flame period and during the period after the volatile flame. *The cumulative quantity for the second period, corresponding with the char oxidation, was not detectable*. Therefore, it can be concluded that it is during the flame period only that PAHs are formed. The char oxidation does not generate significant PAH emissions. We remind at this point that the PAH quantities reported in this work are those formed inside the flame. These initial PAH are likely, in the case of an industrial furnace, to change, as interactions with other gas species will occur.

The influence of the brick density on the total amount of PAH formed during the combustion can be estimated from Fig. 13. From this figure, the accuracy of the PAH quantification can be estimated at ± 5 μg g brick^{-1}. The error might seem large at this point, but we will see in the following that it is largely acceptable for our interpretations. These results show that the density of the brick has not a significant impact on PAH emissions. The average quantity is approximately 10 μg g brick^{-1}.

Fig. 14 gives the total PAH emissions as a function of the element size. *No significant effect of the size of the elements can be observed*. This result is not obvious since it might have been expected that the pore-scale characteristics would have affected the mixing of the volatile matters emitted by the different phases, i.e. PE and cardboard. It should be noticed that this result is established for a domain where only little quantities of PAH are generated, and this should not be extrapolated without experimental validation to bricks containing larger quantities of PE.

Let us consider now the important question of the *quantity of PAH* resulting from the combustion of bricks with various PE percentages. The plot in Fig. 15 gives the total quantity of PAH formed versus the percentage of PE in the brick. At this point, we may return to the question of the

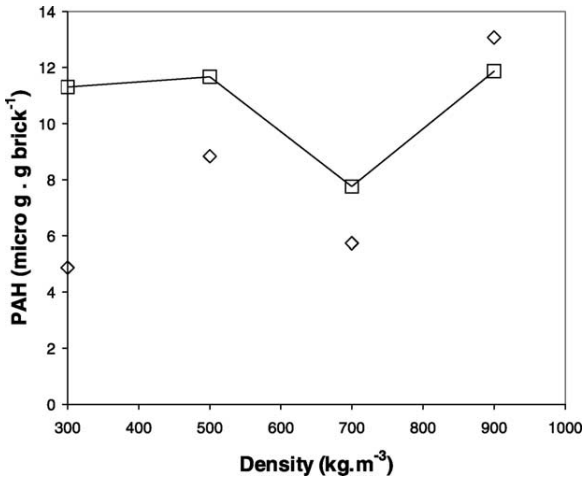

Fig. 13. Total PAH quantity formed during the combustion of bricks with different densities.

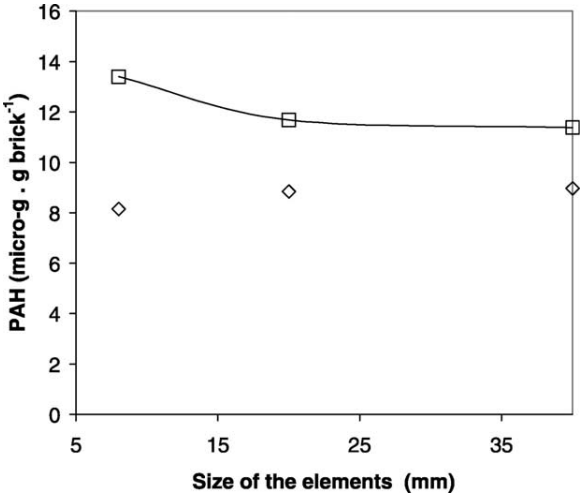

Fig. 14. Total PAH quantity formed during the combustion of bricks with different sizes of the elements.

PAH quantification error and conclude that it is largely acceptable regarding the values involved. Our results clearly shows that very important quantities of PAH can be formed, up to 250 μg g brick^{-1} at high PE concentrations to be compared with 10 μg g brick^{-1} for a brick at 20% PE.

Pure cardboard (0% PE) appears to be responsible for very small PAH formation, <10 μg g brick^{-1}. On the contrary, PE is clearly the material responsible for PAH formation in these experiments. This is consistent with the results from the literature discussed before. Keränen et al. [2] found that, if the fuel contained more than 5% plastic by weight, the level of organic compounds would exceed that from wood burning alone. The present results confirm this finding, even though there is no marked change around the value of 5%.

May these results be interpreted by a concentration based, linear combination of the pure substances PAH production? This would indicate that the mixing has no specific influence on the PAH emission. The dotted line plotted in the figure is

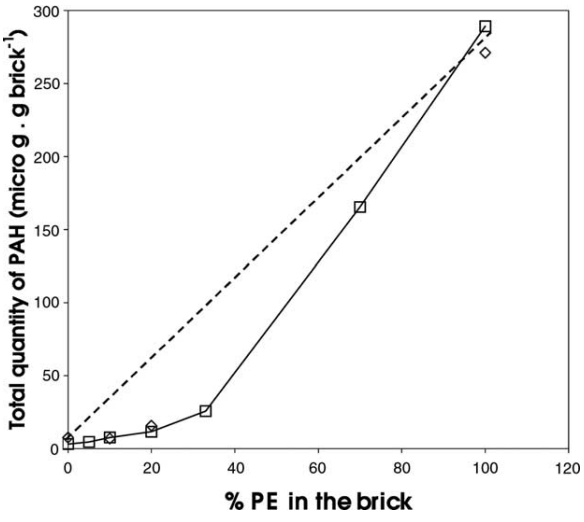

Fig. 15. Total PAH quantity formed during the combustion of bricks with different PE percentages.

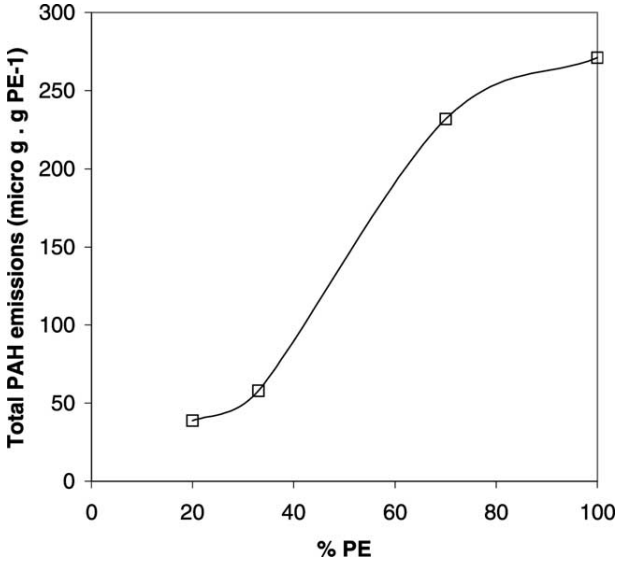

Fig. 16. Total PAH quantity formed during the combustion of bricks with different PE percentages, converted to μg g PE^{-1}.

an interpolation between the quantity of PAH formed during the combustion of cardboard and the quantity formed during the combustion of pure PE. During the combustion of a mix of the two materials, if no interaction did occur, the PAH emissions for a given percentage of PE would be given by this linear interpolation curve. The experiments in this work show that the PAH quantity can be *largely below this curve*. In order to emphasize this point, we have plotted in Fig. 16 the total PAH emissions versus the percentage of PE in the brick, but this time converted into micrograms per gram PE^{-1}, as given in Table 3. These emissions were calculated assuming that cardboard produces 10 μg g $cardboard^{-1}$, and that the complement is due to PE combustion. The curve clearly shows that, above approximately 33% of PE, the quantity of PAH dramatically increases, and reaches, when pure PE is burnt, more than six times the quantity formed when the same mass of PE is mixed with more than 80% of cardboard.

Another important consideration lies in the types of PAH that are produced. This is very interesting since heavy PAH,

Table 3
Quantities of light PAH, of heavy PAH, and total quantity of PAH formed during the combustion of the bricks

PE (%)	PAH (μg g brick-1)			Heavy/light (g g^{-1})	Total PAH (μg g PE^{-1})
	0–3 aromatic rings	4–6 aromatic rings	Total		
0	4.08	3.51	7.59	0.86	
5	2.68	2.05	4.73	0.77	
10	4.03	3.49	7.52	0.86	
20	10.20	5.54	15.74	0.54	38.69
33	6.52	19.30	25.81	2.96	57.92
70	40.67	124.56	165.23	3.06	231.75
100	63.69	207.29	270.98	3.25	270.98

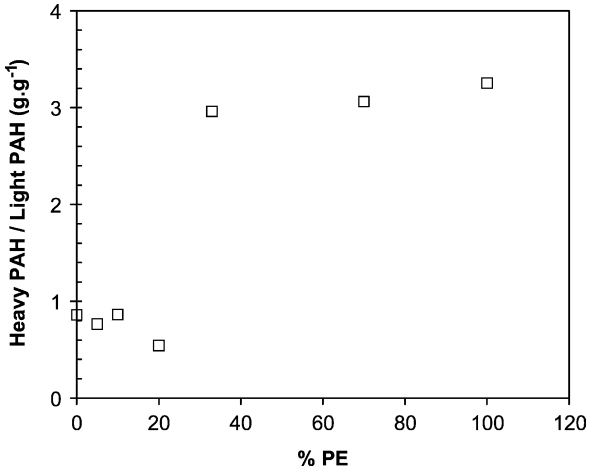

Fig. 17. Mass ratio between heavy PAH and light PAH formed during the combustion of bricks with different PE percentages.

e.g. containing more than three aromatic rings, are more toxic than light PAHs. We have plotted in Fig. 17 the mass ratio between heavy and light PAH versus the PE percentage. For up to 20% PE, the mass of light PAH is lower than that of heavy PAH. With 33% of PE, and for all the bricks with higher PE percentages, there are approximately three times heavier PAH than light PAH. These results show that, in the conditions where large quantities of PAH are formed, the occurrence of heavy PAH is increased. In conclusion, regarding the emission of PAH pollutants, it can be *recommended to introduce less than* 30% *of PE* in a brick.

5. Conclusion

We have demonstrated that it is possible to control in the laboratory the making parameters of a substitution fuel made of mixes of cardboard and plastic. Quantitative data are given in the article concerning the mechanical pressure required in order to reach a given density largely covering those of an industrial production. The calorimeter cone, after simple adaptations, proved to be a suitable device to operate the combustion and to determine with a very good repeatability the total mass information and gas analyses. Thanks to this procedure, the impact on combustion of three brick making parameters has been investigated over ranges largely covering those of an industrial process.

Two of the parameters studied in this work, namely, the density and the percentage of PE, have important impacts on the combustion process. On the contrary, it was found that the size of the elements, in the range 8–40 mm, has little influence.

The maximum temperatures inside the fuel body during the combustion lie within the range 700–900 °C. These levels are very similar, whatever the position below the irradiated surface, and whatever the density of the fuel. As a consequence, it can be inferred from these values that 'NO' thermal formation is likely not to occur inside the brick.

As far as the combustion velocity is concerned, we have observed that the combustion of at least 50 mm thick samples can be separated into two distinct phases, whatever the brick density and composition:

- The first phase, corresponding to devolatilization, is accompanied by the formation of a volatile flame attached to the sample surface. We have observed that this phase duration strongly depends on the density of the fuel, with a linear dependence that has been quantified. The mass loss rate during this phase is very similar from one fuel to another over the whole parameter range, and is always about 6.2×10^{-3} kg s^{-1} m^{-2}.
- The second phase, during which the char residue left after devolatilization oxidizes, is accompanied by mass loss rates again very similar for all the fuels, with values close to 6.0×10^{-4} kg s^{-1} m^{-2}. This is approximately 10 times slower than during the devolatilization phase.

Only few elements for the interpretation in terms of the involved physical phenomena can be given at this stage. This will be investigated in future work by developing a 1D model for the heterogeneous combustion of the mix. The model validation will be possible by a comparison with the 1D experimental results presented in this article.

This work brings some key understanding for the limitation of PAH pollutant emissions when burning plastic materials. We have confirmed that PE will form large quantities of PAH if burnt as a pure material, while PAH emissions from cardboard are more than one order of magnitude lower. PAH are formed during the period where a flame is present at the surface of the sample. We remind at this point that PAH emissions are known to depend strongly on the local stoichiometry inside the flame zone, and on the flame temperature. For an extrapolation to a real industrial process, the results reported here should be considered more as tendencies than absolute values.

In any case, it was found that *mixing PE with cardboard enables to reduce the PAH emissions*. For the conditions operated here, 30% of PE appears to be the recommended maximum proportion. Above this, both the quantity of PAH per gram of PE and the ratio heavy PAH/light PAH will largely increase. In addition, it was found that the density of the fuel and the size of the elements have no significant effect on PAH emissions.

All the results reported here were established for a given radiative heat flux on the surface of the samples, at a value of 50 kW m^{-2}. It is clear that this boundary condition can be different in an industrial process. Nevertheless, we believe that the tendencies observed for the changes in mass loss rate and temperature levels with respect to the studied making parameters can be extrapolated to industrial processes.

Finally, we remind the reader that the end of the combustion process was not studied in this work. The total duration for the combustion of such fuels in an industrial process is mainly governed by surface ash ablation caused by air flows or mechanical strains resulting from handling (grids, rotating drums,…). It was behind the scope of this work to study this phenomenon.

Acknowledgements

We would like to thank Fire Testing Technology Ltd (UK) and B. Auduc (EMAC) for their technical support during the project, and ADEME for funding part of the work.

References

[1] Liu H, Li Y. Compacting municipal solid waste into 'loggs' for combustion at coal-fired power plants. In: Cheng P, editor. Proceedings of the Symposium on Energy in the 21st Century, January, Hong Kong, vol. 4. New York: Begell House; 2000. p. 1420–6.

[2] Keränen E, Aittola J-P, Leppänen A. Combustion of wood and plastic wastes from packaging industry in residential furnaces. Energy Environ Prog I 1991;D:517–31.

[3] Boavida D, Abelha P, Gulyurtlu I, Cabrita I. Co-combustion of coal and non-recyclable paper and plastic waste in a fluidised bed. Fuel 2003;82:1931–8.

[4] Ross AB, Jones JM, Chaiklangmuang S, Pourkashanian M, Williams A, Kubica K, Anderson JT, Kerst M, Danihelka P, Bartle KD. Measurement and prediction of the emission of pollutants from the combustion of coal and biomass in a fixed bed furnace. Fuel 2002;81: 571–82.

[5] Rasmussen I, Overgaard P. General overview over recent results and plans concerning co-combustion of biomass and coal. Fuel Energy Abstr 1997;38(6):471.

[6] Piao M, Chu S, Zheng M, Xu X. Characterization of the combustion products of Polyethylene. Chemosphere 1999;39(9):1497–512.

[7] Panagiotou T, Levendis YA. The effect of the bulk equivalence ratio on the PAH emissions from the combustion of PVC, poly(styrene), and poly(ethylene). 26th Symposium (International) on Combustion, The Combustion Institute; 1996. p. 2421–30.

[8] Lewin M, Basch A, Shaffer B. Studies on the pyrolysis of polymer blends: pyrolysis of cellulose–wool blends. Cellulose Chem Technol 1990;24:417–24.

[9] McGhee B, Norton F, Snape CE, Hall PJ. The copyrolysis of poly(vinylchloride) with cellulose derived materials as a model for municipal waste derived chars. Fuel 1995;74(1):28–31.

[10] Williams PT, Williams EA. Interactions of plastics in mixed-plastics pyrolysis. Energy Fuels 1999;13:188–96.

[11] Babraukas V. Development of the cone calorimeter—a bench scale heat release rate apparatus based on oxygen consumption. Fire Mater 1984;8(2):81–95.

[12] Horttanainen M. Propagation of the ignition front against air flow in packed beds of wood particles. Thesis. Finland: Lappeenranta University of Technology; November 2001.

[13] Freeman DJ, Cattell FCR. Wood burning as a source of atmospheric polycyclic aromatic hydrocarbons. Environ Sci Technol 1990;24: 1581–5.

[14] Van dell RD, Mahle NH, Hixson EM. The effect of oxygen on the formation and destruction of the products of incomplete combustion from the combustion of polyethylene and *o*-dichlorobenzene. Combust Sci Technol 1994;101:261–83.

[15] Longwell JP. The formation of polycyclic aromatic hydrocarbons by combustion. 19th Symposium (International) on Combustion, The Combustion Institute; 1982. p. 1339–50.

[16] Frenklach M. On the driving force of PAH production. 22nd Symposium (International) on Combustion, The Combustion Institute; 1988. p. 1075–82.